Clim. Past, 8, 191–203, 2012
www.clim-past.net/8/191/2012/
doi:10.5194/cp-8-191-2012

Climate of the Past

Towards orbital dating of the EPICA Dome C ice core using $\delta O_2/N_2$

A. Landais[1,*], G. Dreyfus[1,2,*,***], E. Capron[1,**], K. Pol[1], M. F. Loutre[3], D. Raynaud[4], V. Y. Lipenkov[5], L. Arnaud[4], V. Masson-Delmotte[1], D. Paillard[1], J. Jouzel[1], and M. Leuenberger[6]**

[1]Institut Pierre-Simon Laplace/Laboratoire des Sciences du Climat et de l'Environnement, CEA-CNRS-UVSQ – UMR8212, 91191, Gif-sur-Yvette, Franc
[2]Department of Geosciences, Princeton University, Princeton, NJ 08540, USA
[3]Université catholique de Louvain, Earth and Life Institute, Georges Lemaître Centre for Earth and Climate Research (TECLIM), Chemin du cyclotron, 2, 1348 Louvain la Neuve, Belgium
[4]Laboratoire de Glaciologie et Géophysique de l'Environnement, CNRS-UJF, 38402 St. Martin d'Hères, France
[5]Arctic and Antarctic Research Institute, 38 Bering street, St. Petersburg 199397, Russia
[6]Climate and Environmental Physics, Physics Institute, and Oeschger Centre for Climate Change Research, University of Bern, Sidlerstrasse 5, 3012 Bern, Switzerland
[*]now at: Oak Ridge Institute for Science and Education Climate Change Policy and Technology Fellow with the US Department of Energy Office of Policy and International Affairs, 1000 Independence Avenue SW, Washington, DC 20585, USA
[**]now at: British Antarctic Survey, High Cross, Madingley Road, Cambridge, CB3 0ET, UK
[***]These authors contributed equally to this work.

Correspondence to: A. Landais (amaelle.landais@lsce.ipsl.fr)

Received: 24 June 2011 – Published in Clim. Past Discuss.: 30 June 2011
Revised: 7 November 2011 – Accepted: 12 December 2011 – Published: 31 January 2012

Abstract. Based on a composite of several measurement series performed on ice samples stored at −25 °C or −50 °C, we present and discuss the first $\delta O_2/N_2$ record of trapped air from the EPICA Dome C (EDC) ice core covering the period between 300 and 800 ka (thousands of years before present). The samples stored at −25 °C show clear gas loss affecting the precision and mean level of the $\delta O_2/N_2$ record. Two different gas loss corrections are proposed to account for this effect, without altering the spectral properties of the original datasets. Although processes at play remain to be fully understood, previous studies have proposed a link between surface insolation, ice grain properties at close-off, and $\delta O_2/N_2$ in air bubbles, from which orbitally tuned chronologies of the Vostok and Dome Fuji ice core records have been derived over the last four climatic cycles. Here, we show that limitations caused by data quality and resolution, data filtering, and uncertainties in the orbital tuning target limit the precision of this tuning method for EDC. Moreover, our extended record includes two periods of low eccentricity. During these intervals (around 400 ka and 750 ka), the matching between $\delta O_2/N_2$ and the different insolation curves is ambiguous because some local insolation maxima cannot be identified in the $\delta O_2/N_2$ record (and vice versa). Recognizing these limitations, we restrict the use of our $\delta O_2/N_2$ record to show that the EDC3 age scale is generally correct within its published uncertainty (6 kyr) over the 300–800 ka period.

1 Introduction

While ice core records offer a wealth of paleoclimatic and paleoenvironmental information, uncertainties associated with ice core dating limit their contribution to the understanding of past climate dynamics. Absolute age scales have been constructed for Greenland ice cores thanks to layer counting in sites offering sufficient accumulation rates (GRIP, GISP2, NorthGRIP; Rasmussen et al., 2006; Svensson et al., 2006, 2008), allowing the construction of the GICC05 Greenland age scale currently spanning the past 60 ka (i.e. thousand of years before present, present being year 1950 AD in our study). While layer counting is not possible for deep Antarctic ice cores obtained in low accumulation areas, the transfer

of the GICC05 age scale (using gas synchronization methods; e.g. Blunier et al., 2007) to Antarctic records allows researchers to partly circumvent this difficulty for the past 60 ka. Absolute time markers are generally lacking for these long Antarctic records, now extending up to 800 ka, with the exception of promising studies using Ar/Ar and U/Th dating tools (Dunbar et al., 2008; Aciego et al., 2010) and the links between ^{10}Be peaks and well dated magnetic events (Raisbeck et al., 2007). As a result, dating of the deepest part of these Antarctic cores is largely based on various approaches combining an ice flow model with orbital tuning. Classically, orbital tuning assumes that northern hemisphere summer insolation drives large climate transitions (e.g. Milankovitch, 1941), and has long been used for dating paleoclimatic records, especially marine ones (e.g. Martinson et al., 1987).

As for Antarctic ice cores, two different orbital dating approaches, initially developed by Bender et al. (1994) and Bender (2002), are now commonly used. First, long records of δ^{18}O of atmospheric O_2 ($\delta^{18}O_{atm}$) have revealed that this parameter is highly correlated with insolation variations in the precession band with a lag of about 5–6 kyr (thousands of years) (Bender et al., 1994; Petit et al., 1999; Dreyfus et al., 2007). Studies have linked variations in precession to $\delta^{18}O_{atm}$ through changes in low latitude water cycle and biospheric productivity (Bender et al., 1994; Malaizé et al., 1999; Wang et al., 2008; Severinghaus et al., 2009; Landais et al., 2007, 2010). The significant time delay between changes in precession and changes in $\delta^{18}O_{atm}$ has been attributed to a combination of the 1000–2000 year residence time of O_2 in the atmosphere (Bender et al., 1994; Hoffmann et al., 2004) and to the numerous and complex processes linking the isotopic composition of seawater to atmospheric oxygen via the dynamic response of the tropical water cycle to precession forcing and the associated variations in terrestrial and oceanic biospheres (Landais et al., 2010, and references therein). This superposition of processes also suggests that lags may vary with time (Jouzel et al., 2002; Leuenberger, 1997). As a consequence, the $\delta^{18}O_{atm}$ record from long ice cores can be used to constrain ice core chronologies (e.g. Petit et al., 1999; Shackleton, 2000), but with a large associated uncertainty (6 kyr) (Petit et al., 1999; Dreyfus et al., 2007). In parallel, the link between precession, low latitude hydrology, and atmospheric methane concentration (Chappellaz et al., 1993) has been used to propose an orbital age scale for Vostok (Ruddimann et al., 2003). However, past methane variations exhibit a strong impact from obliquity (Loulergue et al., 2008) and a weaker correlation with precession than $\delta^{18}O_{atm}$ (Schmidt et al., 2004; Landais et al., 2010), hence limiting this approach.

Second, Bender (2002) has proposed that the elemental ratio $\delta O_2/N_2$ in the trapped air could be used as a new orbital tuning tool. Indeed, $\delta O_2/N_2$ measurements in the firn near the pore close-off depth (about 100 m below the ice-sheet surface, i.e. where unconsolidated snow is compressed to the density of ice) have revealed that the trapping process is associated with a relative loss of O_2 with respect to N_2 (Battle et al., 1996; Severinghaus and Battle, 2006; Huber et al., 2006). Between 160 and 400 ka, the $\delta O_2/N_2$ record of the Vostok ice core displays variations similar to those of the local 21 December insolation (78° S). From these two observations, Bender (2002) formulated the hypothesis that local Antarctic summer insolation influences near-surface snow metamorphism and that this signature is preserved during the firnification process down to the pore close-off depth, where it modulates the loss of O_2. From this hypothesis, he proposed the use of $\delta O_2/N_2$ for dating purposes.

Despite a limited understanding of the physical mechanisms linking local 21 December insolation and $\delta O_2/N_2$ variations in polar ice cores, this approach has been used by Kawamura et al. (2007) and Suwa and Bender (2008a) to propose an orbital dating of the Dome F and Vostok ice cores back to 360 and 400 ka, respectively. The validity of the link with local summer insolation has been supported by a similar correspondence observed in the Greenland GISP2 ice core (Suwa and Bender, 2008b). Using their high quality $\delta O_2/N_2$ record on the Dome F ice core and comparison with radiometric dating obtained on speleothem records, Kawamura et al. (2007) estimated the dating uncertainty to be as low as 0.8–2.9 kyr. Moreover, it was suggested that, combined with an inverse glaciological modeling approach, the dating uncertainty could be pinched down to 1 kyr (Parrenin et al., 2007).

Up to now, the oldest ice core climatic and greenhouse gases records have been obtained from the EPICA Dome C (EDC) ice core that covers the last 800 ka (Jouzel et al., 2007; Lüthi et al., 2008; Loulergue et al., 2008). The state-of-the-art dating of the EDC ice core (EDC3 chronology) has been described in Parrenin et al. (2007). It is based on ice flow modeling using an inverse method constrained by available age markers. These age markers include reference horizons such as volcanic horizons (Mt Berlin eruption, 92.5 ka; Dunbar et al., 2008) and peaks in ^{10}Be flux (i.e. Laschamp event, 41.2 ka; Yiou et al., 1997; Raisbeck et al., 2008). Other tie points have been introduced based on the comparison of the ice core records with records of other well dated archives: as an example, the abrupt methane increase at Termination 2 was assumed to be synchronous (within 2 kyr) with the abrupt δ^{18}O of calcite (speleothem) shift recorded in Chinese (Yuan et al., 2004) and Levantine (Bar-Mathews et al., 2003) regions at around 130.1 ka. For the last 42 ka, the EDC3 age scale was synchronized with the layer-counted Greenland GICC05 chronology (Svensson et al., 2008). For ice older than the last interglacial period, tie points are exclusively derived from orbital tuning. In addition to 37 $\delta^{18}O_{atm}$ tie points used between 400 and 800 ka, additional orbital information was derived from local insolation changes imprinted in the record of total air content in polar ice. Raynaud and colleagues (2007) indeed showed that the majority of the variance in total air content in the EDC ice core can

be explained by the variations of an integrated summer insolation parameter (i.e. summation of the daily insolation over a certain threshold for a given latitude) that has a dominant obliquity component. This marker was therefore suggested as another tool for orbital dating of ice core records. Moreover, the study by Lipenkov et al. (2011) shows that the two air content and $\delta O_2/N_2$ local insolation proxies lead to orbital timescales that agree to within less than 1 kyr on average.

Ten such "air content" tie points have been used between 71 and 431 ka for EDC3, assuming a 4 kyr uncertainty to account for the scatter in the raw data and the uncertainty due to the choice of the integrated summer insolation target (threshold value for daily insolation). The overall uncertainty attached to the EDC3 time-scale is estimated at 6 kyr from 130 ka down to the bottom of the record. As a result, the uncertainty on event durations can reach 40 % between 400 and 800 ka (i.e. over the period mainly constrained by $\delta^{18}O_{atm}$ orbital tuning) (Parrenin et al., 2007).

In this article, we present the first records of $\delta O_2/N_2$ measured on the EDC ice core between 800 and 300 ka. This record is of special interest since (1) no $\delta O_2/N_2$ data were used for constraining the EDC3 age scale, and (2) no $\delta O_2/N_2$ data have been published to date prior to 410 ka. Our record includes two periods of low eccentricity, centered at around 400 ka and around 750 ka, characterized by a minimum influence of precession variations on insolation (Loutre and Berger, 2003). This contrasts with the relatively large eccentricity context for the time interval between 50 and 360 ka, where previous $\delta O_2/N_2$ records were obtained. Our $\delta O_2/N_2$ record was therefore used for examining (1) the feasibility of orbital dating (in particular with $\delta O_2/N_2$) at times of low eccentricity, and (2) the validity of the EDC3 age scale between 300 and 800 ka with respect to the $\delta O_2/N_2$ constraints.

We first present the analytical methods used to perform the measurements, as well as discuss the effects of gas loss associated with ice storage on the integrity of the $\delta O_2/N_2$ record and the necessary corrections. The spectral properties of the resulting composite EDC $\delta O_2/N_2$ curve are then analyzed with respect to the orbital forcing. The local insolation influence on this EDC signal is compared with previous studies on the Vostok and Dome F ice cores (Bender, 2002; Kawamura et al., 2007; Suwa and Bender, 2008a). Finally, the uncertainties and limitations attached to the use of $\delta O_2/N_2$ as a dating tool for the EDC ice core between 300 and 800 ka are discussed.

2 Methods

2.1 Technique used at LSCE for obtaining the EDC $\delta O_2/N_2$ record

The technique used at the Laboratoire des Sciences du Climat et de l'Environnement (LSCE) for extracting the air trapped in ice core samples is based on melting and refreezing ice samples as first developed by Sowers et al. (1989) and detailed in Landais et al. (2003). For each depth, two adjacent ice samples covering the same depth interval were cut from the ice core. Approximately 3–5 mm of the outer ice was shaved off each face to yield two 10 g ice samples. The samples were placed in pre-cooled glass flasks with glass/metal transitions to Conflat flange tops. The flasks were connected to a vacuum manifold using gold-plated copper gaskets. The manifold is equipped with a Pfeiffer-Balzar turbo molecular pump, two pressure gauges (Baratron, Pirani), manual Nupro valves and 6 ports. Typically, we processed 6 samples per day with this method in two batches of three samples. Following a leak test, the ambient air surrounding the ice samples was evacuated using the turbo-molecular pump for 35–40 min while the ice was kept frozen by immersing the flask in a −20 °C ethanol bath. The flask was then isolated using a manual Nupro valve, and the ice was allowed to melt at room temperature. Once the samples were completely melted, we began refreezing the first sample. Since only one sample can be cryogenically transferred at a time, the samples were refrozen sequentially. Refreezing was accomplished using a 10 cm long copper cold finger with flat top plate placed in contact with the bottom of the sample flask. Only the bottom 3 cm of the cold finger were initially immersed in liquid nitrogen. Heat transfer was facilitated by adding alcohol to the top plate in contact with the flask bottom. This arrangement allowed the melt water to refreeze slowly from the bottom, minimizing the capture of dissolved gases. Cracking of the ice signals refreezing was complete, at which time we completely immersed the cold finger in liquid N_2. In order to remove residual water vapor from the headspace, we heated the metal flange connection with a heat gun for 2.5 min, then maintained the cold finger maximally immersed in liquid N_2 for an additional 10 min, a procedure that ensures that the sample flask is never in direct contact with liquid N_2. The headspace gases were then cryogenically transferred into a quarter inch steel tube plunged into liquid He for 6 min. The gases in the stainless steel tube were allowed to come to room temperature and equilibrate for a minimum of 40 min before being introduced into the mass spectrometer for isotopic and elemental analysis using a dual inlet system.

The measurements of $\delta O_2/N_2$ on the EDC ice core were performed on two different mass spectrometers. The Series 1 (Table 1, Fig. 1) was obtained on a 4-collector Finnigan MAT 252. On this mass spectrometer, the masses (*m/z* 32 (O_2) and 28 (N_2) could not be measured simultaneously. so peak jumping (jumping from one mass to the other) was used to measure $\delta O_2/N_2$. The measurement Series 2, 3 and 4 (Table 1, Fig. 1) were measured on a 10-collector Thermo Delta V Plus that permitted simultaneous acquisition of *m/z* 32 and 28. A careful inter-comparison of the performances of the two mass spectrometers using air standard and firn air on the two instruments showed no significant offsets (Dreyfus, 2008).

Table 1. Details of the 4 different series of $\delta O_2/N_2$ data measured at LSCE (Laboratoire des Sciences du Climat et de l'Environnement) on the EDC ice core (see also Fig. 1). We indicate the number of the series as referenced in the text, the number of depth levels studied, the mean depth interval, the mass spectrometer on which the $\delta O_2/N_2$ measurements were carried out, the year when the analyses were performed, the pooled standard deviation, and the numbers of depth levels rejected associated with each series. Series 1 and 2 were obtained from ice stored at −25 °C, while Series 3 and 4 were obtained from ice stored at −50 °C.

Series	Depth levels	Depth resolution	Mass Spectrometer	Year (AD)	Pooled standard deviation (‰)	Number of outliers
1 (red)	109	3 to 4 m between 2483–2850 m 20 m between 2850–3100 m	Finnigan MAT 252	2005	1.2	10
2 (green)	112	20 m between 2800–3040 m 1.5 m between 3040–3200 m	Thermo Delta V Plus	2006	1.96	23 (14 below 3100 m depth)
3 (blue)	30	2.5 m between 2822–2893 m	Thermo Delta V Plus	2007	0.32	0
4 (purple)	29	2.5 m between 3105 and 3188 m	Thermo Delta V Plus	2008	1.03	0

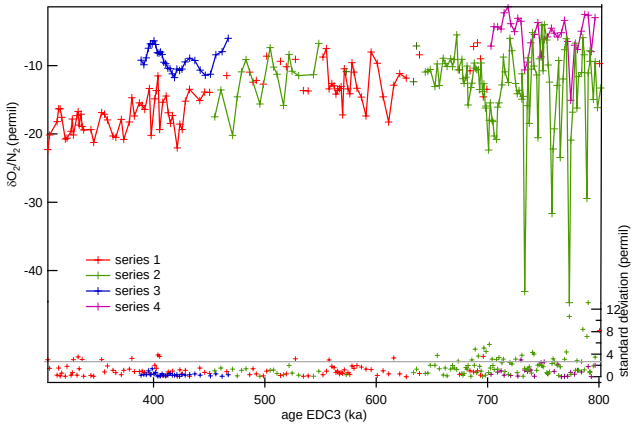

Fig. 1. Measurements of $\delta O_2/N_2$ in the EPICA Dome C (EDC) ice core plotted on the EDC3 ice core age scale (Parrenin et al., 2007) and associated uncertainty (1σ, bottom panel). The EDC $\delta O_2/N_2$ record is composed of four distinct measurement series (top panel). Samples measured in Series 1 and 2 were stored at −25 °C whereas samples measured in Series 3 and 4 were stored at −50 °C. Characteristics of the different series are given in Table 1: Series 1 in red, Series 2 in green, Series 3 in blue, Series 4 in purple.

The method for $\delta O_2/N_2$ measurements at LSCE is similar to the one used for obtaining the Vostok $\delta O_2/N_2$ record (Sowers et al., 1989; Bender, 2002). However, it significantly differs from the one used for the Dome F $\delta O_2/N_2$ record (Kawamura et al., 2007) which requires a much larger ice sample (∼200 g instead of 10 g) and is based on a gas extraction method with no refreezing (Kawamura et al., 2003). No inter-calibration of these different methods has yet been conducted.

2.2 EDC raw data

The measurements have been performed on clathrate ice below 2400 m depth well below the bubble – clathrate transition zone where positive $\delta O_2/N_2$ values have been observed in other records (Bender, 2002). This effect is due to O_2 being more easily dissolved in ice as gas hydrate than N_2, such that after coring, N_2 (from bubbles) is preferentially lost relative to O_2 (from clathrates) in this zone (Bender, 2002; Ikeda-Fukazawa et al., 2005). The complete record is a composite of four different series of measurements from ice with different storage histories (Table 1, Fig. 1). All data have been corrected for gravitational fractionation as follows:

$$\delta O_2/N_2 = \delta O_2/N_{2,\mathrm{raw}} - 4 \times \delta^{15}N. \quad (1)$$

For all series, each sample value corresponds to the average of at least two replicate samples analyzed at each depth level. We then calculated the pooled standard deviation as:

$$\sigma_p = \sqrt{\frac{\sum \left((n_i - 1)\,\sigma_i^2\right)}{\sum (n_i - 1)}} \quad (2)$$

where n_i and σ_i are the sample size and the standard deviation of the i-th sample, respectively. Over the whole set of measurements, σ_p is equal to 1.5 ‰.

As expected from the inter-comparison between the two mass spectrometers, no shift between the mean values appears between the 1st and the 2nd series. The oldest values (700–800 ka) obtained in Series 2 are associated with a large scatter of the $\delta O_2/N_2$ data between neighboring and replicate samples. For two of these depth levels, $\delta O_2/N_2$ reaches extremely low values (lower than −40 ‰) with an associated standard deviation of 10 ‰ (Fig. 1). These ice samples are likely affected by significant gas loss after ice coring that favors the loss of the smaller molecule O_2 with respect to the larger molecule of N_2 (Huber et al., 2006).

On the contrary, samples from Series 3 (stored at −50 °C after ice core drilling instead of at −25 °C) are associated with a very low pooled standard deviation (0.32 ‰) and less scattering than Series 1 and 2. This shows that high precision

$\delta O_2/N_2$ measurements on EDC ice are possible with our experimental set-up if the ice is stored at a very low temperature. Moreover, samples from Series 4, also stored at −50 °C but measured one year later than the samples from Series 3, show a significantly lower scattering than the measurements performed over the same depth range from Series 2 from ice stored at −25 °C. This again confirms the quality of $\delta O_2/N_2$ record from EDC ice samples stored at −50 °C. Still, the uncertainty associated with Series 4 is larger than the one associated with Series 3 despite the fact that the samples were stored under the same conditions. This may be related to the ice history, with warmer temperatures encountered near Dome C bedrock (above −10 °C), to the increased fragmentation of the deepest ice core sections (short fractured cores of ∼20 cm extracted using ethanol as a drilling liquid), or to a change in ice crystal structure at high depths (Pol et al., 2010; Durand et al., 2010).

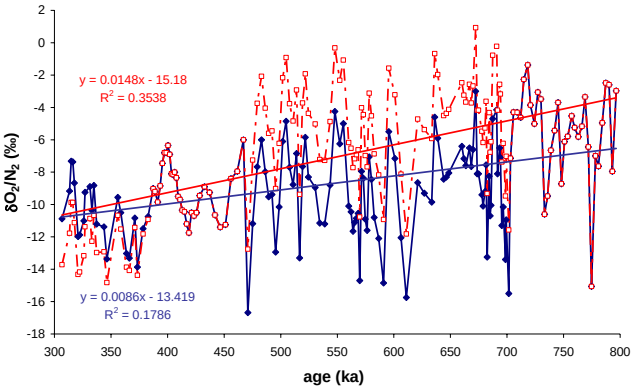

Fig. 2. Two gas loss corrections for the EDC $\delta O_2/N_2$ record. We propose two gas loss corrections since no accurate storage history documentation is available: "gas correction 1" (curve 1 = red) shifts all Series 1 and 2 data by +6.43 ‰ (the average offset between Series 1 and 2 when compared with Series 3), resulting in a variance of 13 ‰ after outlier rejection; "gas correction 2" (curve 2 = blue) seeks to homogenize Series 1 and 2 with Series 3 and 4 where they overlap.

3 Gas loss correction and construction of a composite curve

3.1 Principle of gas loss from air bubbles

Bender et al. (1995) showed anomalously low O_2/N_2 and Ar/N_2 ratios in air extracted from ice cores compared to atmospheric air. This effect was initially attributed to gas loss during coring and storage, with the smallest molecules (O_2, Ar) being more easily lost than the larger ones (N_2). Ikeda-Fukazawa et al. (2005) observed a drift in the O_2/N_2 ratio correlated with the storage duration. Two mechanisms were proposed to explain this size dependent effect: diffusion through the ice lattice by breaking of hydrogen bonds (Ikeda-Fukazawa et al., 2005) or diffusion through small channels in the ice with a threshold dimension of 3.6 Å (i.e. molecules with a diameter larger than 3.6 Å, like N_2, will not escape from the bubbles) (Huber et al., 2006).

For the Dome F ice, Kawamura et al. (2007) found that $\delta O_2/N_2$ decreased by 6.6 ‰ per year of storage at −25 °C, and used this relationship to apply a gas loss correction. While the exact storage temperature histories of our samples are less well known, we observe significant shifts in $\delta O_2/N_2$ levels between samples stored 1–2 years at −25 °C (Series 1 and 2) and samples stored at EDC (−50 °C) and maintained at this temperature during transport and storage (Series 3 and 4) as depicted above.

3.2 Corrections

In order to remove outliers, we excluded all the measurements at depth levels where the $\delta O_2/N_2$ standard deviation associated with replicates is larger than 3 ‰ (Fig. 1). This rejects less than 16 % of the data (mainly over the deepest part of Series 2, see details in Table 1) and results in a pooled standard deviation of 0.9 ‰. This is very comparable to the pooled standard deviation obtained on the $\delta O_2/N_2$ records of the Vostok and Dome F ice cores after gas loss correction and removal of 15 to 20 % of outliers (Bender, 2002; Kawamura et al., 2007; Suwa and Bender, 2008a).

As discussed above, the $\delta O_2/N_2$ measurements performed on ice stored at −50 °C are not appreciably affected by gas loss so that we keep Series 3 and 4 without any correction. Then, we propose a correction that accounts for a systematic bias in the measurements when ice is stored at −25 °C instead of −50 °C. It is based on the following observations: (a) there is no obvious shift between Series 1 (measured in 2004–2005) and 2 (measured in 2006–2007); (b) after an homogenization of Series 1, 2 and 3 through a linear interpolation every 1 kyr between 380 and 480 ka, we found an average offset between Series 1 and 2 on the one hand and Series 3 on the other hand of 6.43 ‰. We thus decided to shift all the $\delta O_2/N_2$ values of Series 1 and 2 by adding 6.43 ‰. We call this "gas loss correction 1".

This correction is subject to discussion. In particular, it leads to a significant decrease in $\delta O_2/N_2$ with time: the mean $\delta O_2/N_2$ level before 480 ka is less depleted than the mean $\delta O_2/N_2$ level after 380 ka (Fig. 2); the variance of the whole record after the rejection of outliers and "gas loss correction 1" is about 13 ‰. We therefore propose an alternate correction, "gas correction 2". This second correction aims to homogenize (1) the mean level of $\delta O_2/N_2$ between Series 2 and Series 4 around 700–750 ka, (1) the mean level of $\delta O_2/N_2$ between Series 1, 2 and Series 3 around 430–480 ka and (3) the mean level of $\delta O_2/N_2$ between Series 1 and Series 3 around 380–430 ka. In order to fulfill requirements (1) and (2), a simple solution is to add 2.5 ‰ to the $\delta O_2/N_2$ of Series 1 and 2 between 430 and 700 ka. Then, in order to fulfill requirement (3), one possible solution (albeit not the only

one) is to apply the following correction to Series 1 and 2 between 300 and 430 ka:

$$\delta O_2/N_2\_corr = \delta O_2/N_2\_uncorr + 2.5 - 0.035 \times (t - 500) \quad (3)$$

where $\delta O_2/N_2$_corr is the corrected $\delta O_2/N_2$, $\delta O_2/N_2$_uncorr is the original $\delta O_2/N_2$ measurements from Series 1 and 2 and t is the age of the $\delta O_2/N_2$ data point in ka. This second correction is different from the first one, being larger for the recent time period (300–430 ka) than for the oldest period (430–700 ka). The choice of the correction will thus have an impact on the magnitude of the long-term trend of $\delta O_2/N_2$.

The final variance of the $\delta O_2/N_2$ record after outlier rejection and "gas loss correction 2" is less than 9 ‰, which is comparable with the variance of the Dome F and Vostok $\delta O_2/N_2$ records.

3.3 Reconstructed curve from EDC $\delta O_2/N_2$

We now construct a composite EDC $\delta O_2/N_2$ record over the period 300–800 ka as follows:

- when Series 1 and 2 overlap with Series 3 and 4, we only keep the measurements from Series 3 and 4.
- we use the two gas loss corrections (outlier correction and gas loss correction) described in the previous paragraph for Series 1 and 2 on the remaining periods.

Because we have two alternative "gas loss corrections", we produce two different composite curves, hereafter curves 1 and 2 (Fig. 2). This provides a means of estimating the effect of our subjective gas loss corrections on the final $\delta O_2/N_2$ record. It should be noted that with such corrections, we do not correct the scattering of $\delta O_2/N_2$ data probably due to small-scale gas loss observed in Series 1 and 2. This scattering is especially visible on the corrected curves between 550 and 600 ka.

An obvious difference between the two composite curves is the temporal evolution of $\delta O_2/N_2$ with time. While curve 1 shows a long-term decrease of $\delta O_2/N_2$ of −0.014 ‰ per kyr, its value is only of −0.008 ‰ per kyr for curve 2 (Fig. 2). The general long-term evolution of $\delta O_2/N_2$ with time is robust with respect to gas loss correction independent of our empirically derived gas loss corrections. This evolution is due to the fact that the average $\delta O_2/N_2$ is higher in Series 4 than in Series 3, and neither of these series have been corrected since they should not be significantly affected by gas loss since they were stored at −50 °C.

For Vostok, a decrease of −0.013 ‰ per kyr was observed between 150 and 400 ka (Bender, 2002; Suwa and Bender, 2008a), while Dome F data (Kawamura et al., 2007) show a smaller negative temporal trend (decrease of −0.006 ‰ per kyr). Given that various gas loss corrections are applied to these different data sets, we cannot assess the origin of this trend, i.e. natural long-term $\delta O_2/N_2$ variability, a gas loss effect, or a pore close-off effect.

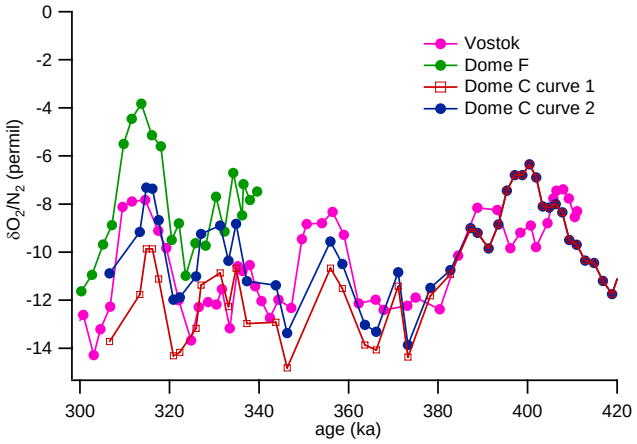

Fig. 3. Comparison between the two composite EDC $\delta O_2/N_2$ curves and existing $\delta O_2/N_2$ records from Dome F (Kawamura et al., 2007) and Vostok (Bender et al., 2002; Suwa and Bender, 2008a). Because of the different time periods covered by the different ice cores, the comparison is limited to the period 300–340 ka for Dome F and EDC and 300–410 ka for Vostok and EDC.

3.4 Comparison with previous $\delta O_2/N_2$ records

Figure 3 compares the two composite curves obtained from our EDC $\delta O_2/N_2$ data and the previous $\delta O_2/N_2$ records from Dome F (Kawamura et al., 2007) and Vostok (Bender et al., 2002; Suwa and Bender, 2008a). Because of the different time periods covered by the different ice cores, the comparison is restricted to the period 300–340 ka for Dome F and EDC and 300–410 ka for Vostok and EDC. A broad agreement is found with the exception of two features. First, the large peak observed around 400 ka on the EDC record appears as a double peak in the Vostok record. We have confidence in the quality and resolution of our measurements over this period because they were performed on ice stored at −50 °C with a pooled standard deviation of 0.32 ‰ and a mean age resolution of 1.5 kyr. Second, the Dome F data are on average less depleted than the Vostok and EDC data. This could be due to differences in the gas loss effect resulting from different stress experienced by each core after coring. However, we have applied our empirical gas loss corrections to the EDC data over the period 300–340 ka, so a future comparison on samples minimally affected by gas loss would be more useful to evaluating such an effect.

4 Spectral properties and link with orbital frequency

4.1 Spectral analysis

The initial $\delta O_2/N_2$data set on the EDC3 age scale over the period 300 to 800 ka is associated with a minimum, average, and maximum sampling step of 1, 2.5 and 6 kyr (the latter only in one extreme case), respectively. The data are

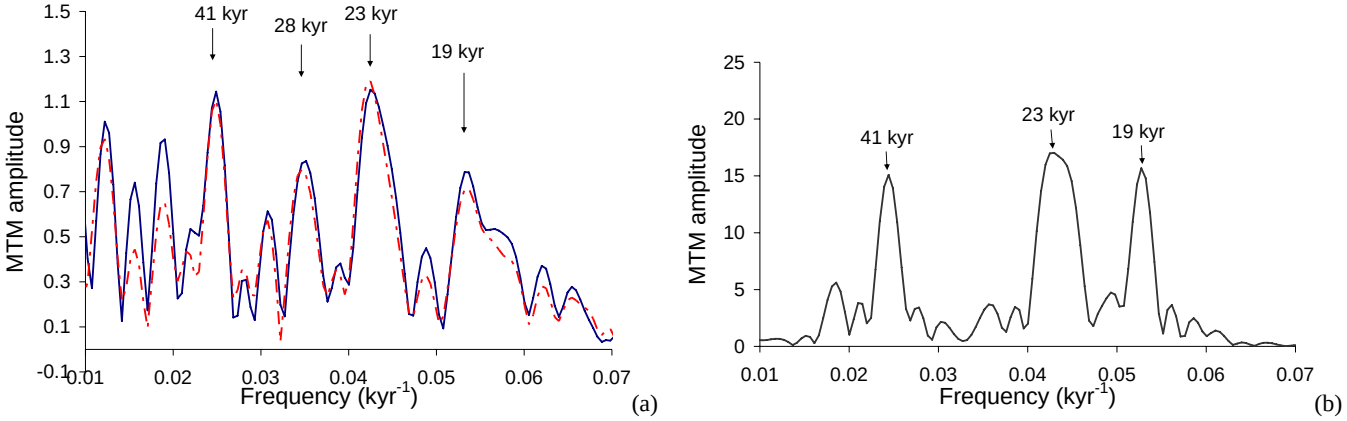

Fig. 4. (a) Spectral analysis (Multi-Taper Method) of the $\delta O_2/N_2$ composite curves (gas loss correction 1 in red and gas loss correction 2 in blue). The significant peaks (>90 %) are identified with an arrow on top. **(b)** Spectral analysis (Multi-Taper Method) of the insolation curve (21 December insolation at 75° S). The significant peaks (>90 %) are identified with an arrow on top.

first interpolated at a constant time step. The Multi-Taper Method, producing a spectrum in amplitude, is then used to identify the major spectral components of the $\delta O_2/N_2$ record. We have checked that the results are robust with respect to the spectral analysis method used, as well as with respect to the resampling. Indeed, the same spectral components were obtained using the Blackman Tukey or Classical FFT (Fast Fourier transform) periodogram methods. Reinterpolating the data at steps of 2 or 3 kyr does not yield significantly different results. These analyses were performed with Analyseries software (Paillard et al., 1996).

For the two corrected curves, we observe the same significant frequency peaks (Fig. 4a). Two large peaks coincide with the frequencies of precession (periods of 23 kyr and 19 kyr). A spectral peak at 41 kyr is associated with obliquity (less prominent with the Blackman-Tukey method). A secondary peak is identified at 28 kyr but its detection depends in the spectral analysis method.

Our results can be compared to spectral analysis of the $\delta O_2/N_2$ records of Vostok over the period 150–400 ka (Bender, 2002) and of Dome F between 82 and 360 ka (Kawamura et al., 2007). They all show the same patterns, a large peak corresponding to a period of 23 kyr and a smaller one corresponding to a period of 41 kyr. We note that neither Vostok nor Dome F $\delta O_2/N_2$ records exhibit a shoulder at 19 kyr.

As already demonstrated in previous studies, the $\delta O_2/N_2$ power spectrum resembles that of local insolation, more precisely the insolation received the 21 December at the Dome C site, with the dominance of precession and obliquity (Fig. 4b). It should be noted that the 19-kyr peak, corresponding to precession frequency, is present both in the spectrum of $\delta O_2/N_2$ from our record between 300 and 800 ka and in local 21 December or monthly mean December insolation spectra over the same period. In contrast, it is less clearly imprinted in both the spectrum of $\delta O_2/N_2$ and in the summer insolation spectrum over the last 400 ka (Bender, 2002; Suwa and Bender, 2008a; Kawamura et al., 2007).

4.2 Impact of data filtering

Filtering the $\delta O_2/N_2$ record reveals the strong correlation with orbital forcing. Following previous studies (Kawamura et al., 2007; Suwa and Bender, 2008a), we performed a data re-sampling with a step of 1 kyr, and the resampled series were band pass filtered based on a fast Fourrier transform (FFT) using a piecewise linear window with sharp slopes at the edges ($<10^{-5}$ kyr^{-1}) (Analyseries software; Paillard et al., 1996). In order to study the link between $\delta O_2/N_2$ and local summer insolation, it is essential that the precession and obliquity frequencies be preserved. Therefore, we chose two different ranges of filtering frequencies corresponding to the following periods: 15–100 kyr and 15–60 kyr (Fig. 5). We applied these filters to both composite curves, and found results similar to the digital filter of Kawamura et al. (2007) (Fig. 5). Like the digital filter described in Kawamura et al. (2007) based on finite duration impulse response, these filters do not significantly affect the position of the peaks of the local insolation curves (position of peaks are not affected by more than 0.15 kyr). However, applying these filters does slightly influence the timing of the EDC $\delta O_2/N_2$ extrema (Fig. 5), which can have important consequences when matching $\delta O_2/N_2$ record with insolation curves.

The time-delays between the filtered $\delta O_2/N_2$ records using both different filtering ranges have been quantified using the cross-wavelet transform technique (Mallat, 1998; Torrence and Compo, 1999) as follows. The cross-wavelet spectrum of two series, computed from the continuous wavelet transform of each series, provides an estimate of the local phase difference between the two series for each point of the time-frequency space. Its integration over a frequency interval allows the computation of the instantaneous time lag between the two series in the corresponding frequency band (Mélice and Servain, 2003). With this method, the time-delays between the filtered $\delta O_2/N_2$ obtained with the different filtering

ranges is of a few centuries (Fig. 5), with the exception of the period 380–450 ka where the shifts can reach 1 kyr.

There are two main causes for the time shifts detected by the different filtering methods: the resolution of the data and the ratio between signal and noise. Tests with resolution ranging from 1 to 5 kyr have shown that peaks can be shifted by a maximum of ±300 yr over the period 300 to 450 ka. Monte-Carlo tests on white noise added to our composite $\delta O_2/N_2$ curve have produced peak displacements of up to ±1.3 kyr (2σ), in particular over the period from 300 to 400 ka. Shifts in peak position from filtering are largest over the period 340–360 ka (small signal and poor resolution), 360–450 ka (small signal) and between 610 and 680 ka (poor resolution). In the following, we consider the $\delta O_2/N_2$ record filtered between 15 and 100 kyr. Because of the time shift in the $\delta O_2/N_2$ extrema discussed above, their position is associated with an uncertainty of 1 kyr between 380 and 450 ka, and 0.5 kyr elsewhere.

In addition to the two effects quantified above, it should be noted that the short-term variations in $\delta O_2/N_2$ due to small-scale gas loss variations can have an effect on the final, filtered curve if the resolution is too low. We should thus consider cautiously the $\delta O_2/N_2$ profile in the low resolution period where the isolated data points may be more affected by this gas loss effect than by the insolation signal. To get a qualitative sense of the validity of the filtered curve, we compare it directly with the original data (Fig. 5). This comparison reveals two periods, i.e. between 610 and 680 ka and between 340 and 360 ka. During these intervals, relatively sparse $\delta O_2/N_2$ coverage and small $\delta O_2/N_2$ variations make the identification and correlation of extrema with the filtered curve ambiguous or impossible. This prevents us from using these data for assessing the quality of the EDC3 chronology.

5 Testing EDC3 using $\delta O_2/N_2$ and local insolation

The previous studies using $\delta O_2/N_2$ in Antarctica (Bender, 2002; Kawamura et al., 2007; Suwa and Bender, 2008a) have compared the $\delta O_2/N_2$ records over the last 400 ka with 21 December insolation or monthly (December) mean insolation at the latitude of each ice core, which display only minor differences. Based on the assumption that the phase lag between $\delta O_2/N_2$ and 21 December insolation is nil as suggested by the Vostok data (Bender, 2002), the new dating of Vostok and Dome F were constructed by matching the peaks of the filtered $\delta O_2/N_2$ curve and of either December (Suwa and Bender, 2008a) or 21 December insolation (Kawamura et al., 2007). In the northern hemisphere, for the Greenland GISP2 ice core, the dating was based on the local summer insolation (June) (Suwa and Bender, 2008b).

To explore the link between our EDC $\delta O_2/N_2$ and local insolation, we have used the 21 December insolation at 75° S computed with Analyseries software (Paillard et al., 1996) using astronomical solution inputs from Laskar (2004).

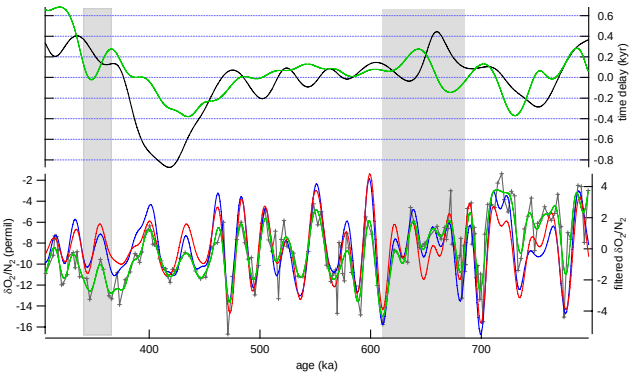

Fig. 5. Effect of band pass filtering of the $\delta O_2/N_2$ record. Bottom panel: composite $\delta O_2/N_2$ data (curve 2, dark grey). Resampled (1 kyr) and filtered $\delta O_2/N_2$ signal with "gas loss correction 2" (i.e. curve 2) for frequencies corresponding to 15–100 kyr (blue) and 15–60 kyr (red). The effect of the Kaiser window filter described in Kawamura et al. (2007) is displayed in green. Top panel: time delay between the filtered curves at 15–100 kyr and at 15–60 kyr (black). The green curve indicates the time delay between the filtered curve at 15–100 kyr and the one using the Kaiser window filter of Kawamura et al. (2007). The grey rectangles indicate the periods when the resolution of the $\delta O_2/N_2$ signal is too low (>3 kyr), limiting the validity of the filtering.

Values were computed with a time step of 1 kyr and then filtered to preserve only the periodicities between 15 and 100 kyr (Fig. 6).

The comparison between our $\delta O_2/N_2$ filtered data (curves 1 and 2) and the insolation target was first explored through a correlation calculation enabling a relative temporal shifting between the series (cross correlation function of Analyseries; Paillard, 1996). Considering the whole record, we got a maximum $R^2 = 0.51$ between our filtered $\delta O_2/N_2$ curve and a mean temporal shift of 2 kyr between the $\delta O_2/N_2$ and insolation curves. To further study this temporal shift, we completed this correlation analysis with a time delay analysis using again the cross wavelet transform technique (Fig. 6). We note several features of this phase analysis. First, we confirmed that the average time delay is 2 kyr between $\delta O_2/N_2$ and insolation 21 December. Second, we observed that the time delays exhibit four maxima at ∼450, ∼550, ∼650 and ∼750 ka. Note that this time delay analysis does not depend on the gas loss corrections.

The variations of the time delays between the EDC $\delta O_2/N_2$ curve and the insolation curve could have several origins/implications:

1. The target curve for $\delta O_2/N_2$ record over 300–800 ka at Dome C should be insolation at another date than 21 December. This is suggested by the significant lag observed at Dome C between the maximum of summer insolation 21 December and the maximum of surface temperature (see Appendix).

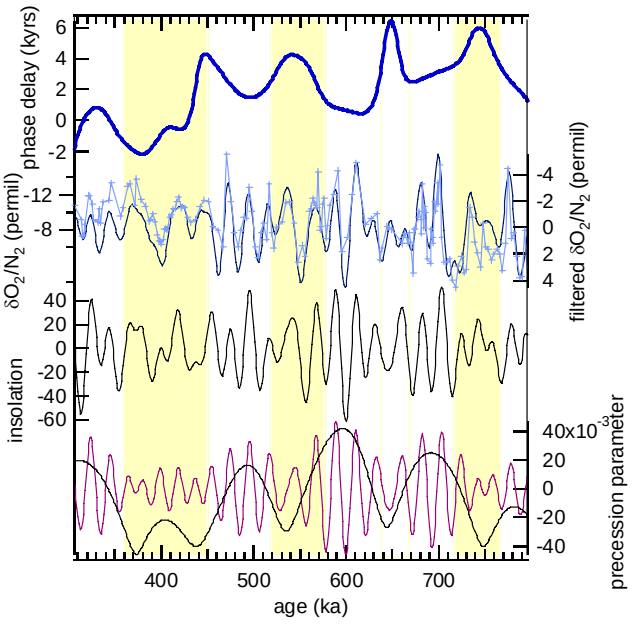

Fig. 6. Possible orbital constraints derived from $\delta O_2/N_2$ record when compared to the local 21 December insolation and precession curves. From top to bottom:

- Time delay between $\delta O_2/N_2$ (curve 2) and local summer insolation curves (21 December insolation at 75° S). The original series were band pass filtered (between 15 and 100 kyr) before the computation of the time delay.
- $\delta O_2/N_2$ curve (curve 2) from the EDC ice core (light blue: raw data; dark blue: after 1 kyr re-sampling and band pass filtering between 15 and 100 kyr). Note the reversed vertical axes.
- 75° S summer insolation on 21 December.
- Precession (purple) and eccentricity (black).

The time periods highlighted in yellow correspond to significant changes in the time delay of $\delta O_2/N_2$ vs. insolation. Time periods with low eccentricity are highlighted in grey.

2. A systematic bias of the EDC3 age scale toward ages that are too old over the 300–800 ka period.

If the problem is in the EDC3 age scale, the correlation and time delays between $\delta O_2/N_2$ and insolation variations enable an independent estimate of the EDC3 age scale uncertainty. Our data suggest that the EDC3 dating is correct within ±2.5 kyr (i.e. 2 kyr due to the average time delay plus 0.5 kyr due to uncertainty in the filtering) over the period 300–800 ka, with the exception of four intervals marked by larger uncertainties. During the periods 390–460 ka, around 550 ka, around 650 ka (we note a lower confidence over this period, as shown in Fig. 5) and around 750 ka, the EDC3 age scale uncertainty could be as high as ±5 kyr (i.e. 4 kyr due to the time delay plus up to 1 kyr due to uncertainty in the filtering method). Such a large uncertainty is still within the uncertainty range of the published EDC3 timescale (±6 kyr) (Parrenin et al., 2007).

We now examine the opportunity to improve the EDC3 age scale by tuning our $\delta O_2/N_2$ record on the insolation curve on 21 December, as has already been done for the Vostok and Dome F ice cores with peak-to-peak correspondence. Such systematic peak-to-peak correspondence is sometimes difficult to identify, in particular during periods with low eccentricity. A first example can be seen over the low eccentricity period between 390 and 460 ka, when the insolation curves display two small peaks or shoulders at 405 and 424 ka (Fig. 6). Neither of these secondary peaks is clearly identifiable in our filtered $\delta O_2/N_2$ signal nor in the original $\delta O_2/N_2$ record. This mismatch cannot be attributed to a deficient quality of our $\delta O_2/N_2$ record since the measurements were performed on ice stored at −50 °C. Another reason may be that small variations of insolation during this period do not have significant impact on the processes controlling $\delta O_2/N_2$. Whatever the causes of such mismatch, the time difference between the two insolation minima on each side of the small peaks reaches up to 20 kyr (for the 405 ka peak). This difference will lead to a tuning uncertainty of up to ±10 kyr over this period, if we match the peaks of the $\delta O_2/N_2$ record with the mid-peaks of the insolation target curve as is classically done. A second example is the minimum of insolation at 750 ka: here the number of peaks is similar between the $\delta O_2/N_2$ and the insolation curves. Still, an unambiguous identification is difficult, as shown by a time delay of 4–5 kyr. In turn, caution should be taken, at least for the EDC record, when tuning $\delta O_2/N_2$ variations to the summer insolation curve over periods of low eccentricity for which high precision (i.e. ice stored at −50 °C) and high resolution $\delta O_2/N_2$ data are needed in any case.

6 Conclusion and perspectives

We have presented the first record of $\delta O_2/N_2$ over the EDC ice core covering the period between 306 and 796 ka. Many samples were stored at −25 °C for 1 year or more before their analysis, such that raw $\delta O_2/N_2$ measurements are strongly affected by gas loss fractionation. Using high precision $\delta O_2/N_2$ measurements performed on similar depths on EDC samples carefully kept frozen at −50 °C, we were able to propose two gas loss corrections to build composite $\delta O_2/N_2$ curves. Using one or another gas loss correction has no significant influence on the orbital chronology issue. However, the band pass filtering method on our $\delta O_2/N_2$ record can lead to an uncertainty of the order of 1 kyr.

The frequency spectrum of EDC $\delta O_2/N_2$ composite curves and of local insolation of 21 December 75° S are very similar over the period 300–800 ka, as previously observed for other ice core $\delta O_2/N_2$ records over the 0–400 ka period. Following previous studies performed on the Vostok and Dome F ice cores over the last 400 ka, we have explored the added value of the $\delta O_2/N_2$ signal to test the EDC3 age scale over the period 300–800 ka. In our case, the time correspondence

of $\delta O_2/N_2$ with 21 December insolation is not so obvious because there is a mean time delay of 2 kyr between our filtered $\delta O_2/N_2$record and the 21 December local insolation. Moreover, we have shown that for low eccentricity time periods, it remains a challenge to identify unambiguously peak-to-peak correspondence between $\delta O_2/N_2$ and insolation. These two effects result in a large uncertainty (more than 10 kyr locally) in the determination of a new chronology, which prevents us from using the current $\delta O_2/N_2$ record to produce a new EDC age scale.

Even if we call for cautiousness in the use of $\delta O_2/N_2$ as an unambiguous dating tool and if this uncertainty prevents us from using our $\delta O_2/N_2$ constraints for building a new EDC age scale, we can still use the comparison between $\delta O_2/N_2$ and the local 21 December insolation to test the current EDC3 chronology. First, we show that over the major part of the 300–800 ka period, EDC3 is correct within the published uncertainty (6 kyr). We identify, however, several specific periods where the shift between $\delta O_2/N_2$ record and the local 21 December insolation signal shows strong variations. These anomalies are observed during periods of low eccentricity and suggest that $\delta O_2/N_2$ cannot be used as dating constraints during minima of eccentricity, or that the EDC3 age scale should be revised over the following periods: 360–450 ka and 720–760 ka.

In order to improve the dating of the oldest Antarctic records (EDC and Dome F), it would be valuable to produce high-accuracy records of total air content, $\delta O_2/N_2$ and $\delta^{18}O_{atm}$ over the period 300–800 ka with a focus on the period 350 to 390 ka to improve our constraint on the length of MIS 11. The consistency of the various records in two ice cores would allow us to establish common and more accurate age scales. Our long $\delta O_2/N_2$ record further reveals that the variance of the signal is preserved back to 800 ka even close to bedrock, and that, if stored at $-50\,^{\circ}C$, deep and old ice can provide accurate $\delta O_2/N_2$ records. This has strong implications for the IPICS (International Partnerships in Ice Core Sciences) oldest ice challenge, with the target to obtain Antarctic ice cores spanning more than one million years and to date them.

Appendix A

Uncomplete understanding of the link between $\delta O_2/N_2$ and local insolation

In this section we explore the possibility that $\delta O_2/N_2$ in the EDC ice core is not solely dependent on 21 December or December insolation (which have very similar spectral properties).

A clear mechanism linking 21 December insolation and $\delta O_2/N_2$ in ice core is not understood. A link has been suggested through seasonal maximum in surface temperature based on the strong link evidenced between 21 December insolation and the seasonal maximum of Dome F surface temperature (with no lag) (Kawamura et al., 2007). However, the timing is different at Dome C with a lag of 15-20 days between the maximum of insolation (21 December) and the surface temperature maximum (Fig. A1).

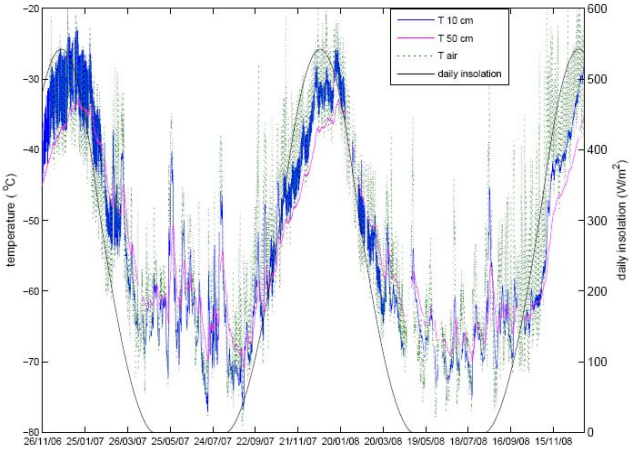

Fig. A1. Evolution of the daily insolation (black), air temperature (dotted green), snow temperature at 10 cm depth (blue) and temperature at 50 cm depth (pink) at the Dome C station between the year 2006 and 2008.

The temperature measurements of the snow at Dome C are part of a more complete system which records temperatures every hour at 40 levels from the surface down to 21 m since November 2006. Temperatures were measured with 100 ohm Platinum Resistance Temperature (PRT) detectors (IEC751 1/10 DIN). A more detailed description of the system and an open data access is available on the OSUG website (http://www.obs.ujf-grenoble.fr). The air temperature sensor is housed in a naturally aspirated, multi-plate radiation shield (Young 41003), and the measurement was performed at 1 m height.

The lag between the maximum of snow temperatures measured at 10 cm and 50 cm is due to the diffusion time of the annual wave temperature between these two levels. The obvious decrease of the diurnal amplitude variations of T_10 cm during the observed period is due to the snow accumulation at the surface. This accumulation implies also an increase of the lag between air and snow temperature measurements.

Recent progresses have been done to improve our understanding of the mechanisms linking surface temperature, snow metamorphism and $\delta O_2/N_2$ (Kawamura et al., 2007). On the one hand, Hütterli et al. (2010) developed a simple model based on the concept that the evolution of temperature gradient metamorphism affects the snow structure in response to local insolation and suggested that significant shifts by several kyr can exist between snow metamorphism and 21 December local insolation. On the other hand, Fujita et al. (2009) measured physical properties of the Dome F firn and studied the density layers evolution during firnification. Based on these results, they proposed a model linking firn properties with conditions for the gas transport processes

near the bottom of firn. This model explains how stronger insolation can lead to bulk ice with a lower $\delta O_2/N_2$.

To conclude, the assumption that $\delta O_2/N_2$ is systematically linked with the 21 December local insolation whatever the climatic conditions at the site and the orbital context deserves further scrutiny.

Acknowledgements. We would like to thank Bénédicte Minster for the help in the measurements as well as Catherine Ritz, Olivier Cattani and Sonia Falourd for the complex logistics involved in cutting and transporting EDC samples at −50 °C from Dome C to our laboratory. We thank Frédéric Parrenin as well as 3 reviewers for constructive comments allowing very significant improvements of this manuscript. Kenji Kawamura is acknowledged for having provided the results of the filtering method described in Kawamura et al. (2007) and applied on our set of data. We also thank Eric Lefebvre for the snow temperature measurement system. This project was funded by the European project EPICA-MIS and the French ANR PICC project. G. Dreyfus acknowledges support from the National Science Foundation Graduate Research Fellowship program and the Commissariat à l'Energie Atomique. This work is a contribution to the European Project for Ice Coring in Antarctica (EPICA), a joint European Science Foundation/European Commission scientific programme, funded by the EU (EPICA-MIS) and by national contributions from Belgium, Denmark, France, Germany, Italy, the Netherlands, Norway, Sweden, Switzerland and the UK. The main logistic was provided by IPEV and PNRA (at Dome C) and AWI (at Dronning Maud Land). This is a contribution to the European project PAST4FUTURE. This is LSCE contribution no. 4334.

Edited by: M. Siddal

The publication of this article is financed by CNRS-INSU.

References

Aciego, S., Bourdon, B., Schwander, J., Baur, H., and Forieri, A.: Toward a radiometric ice clock : U-series of the Dome C ice core, TALDICE-EPICA science meeting, Rome, Italy, 12–15 April 2010.

Bar-Matthews, M., Ayalon, A., Gilmour, M., Matthews, A., and Hawkesworth, C. J.: Sea-land oxygen isotopic relationships from planktonic foraminifera and speleothems in the Eastern Mediterranean region and their implication for paleorainfall during interglacial intervals, Geochim. Cosmochim. Acta, 67, 3181–3199, 2003.

Battle, M., Bender, M. L., Sowers, T., Tans, P. P., Butler, J. H., Elkins, J. W., Ellis, J. T., Conway, T., Zhang, N., Lang, P., and Clarke, A. D.: Atmospheric gas concentrations over the past century measured in air from firn at the South Pole, Nature, 383, 231–235, 1996.

Bender, M. L.: Orbital tuning chronology for the Vostok climate record supported by trapped gas composition, Earth Planet. Sc. Lett., 204, 275–289, 2002.

Bender, M., Sowers, T., and Labeyrie, L.: The Dole effect and its variations during the last 130,000 years as measured in the Vostok ice core, Global Biogeochem. Cy., 8, 363–376, 1994.

Blunier, T., Spahni, R., Barnola, J.-M., Chappellaz, J., Loulergue, L., and Schwander, J.: Synchronization of ice core records via atmospheric gases, Clim. Past, 3, 325–330, doi:10.5194/cp-3-325-2007, 2007.

Chappellaz, J., Blunier, T., Raynaud, D., Barnola, J.-M., Schwander, J., and Stauffer, B.: Synchronous Changes in Atmospheric CH_4 and Greenland Climate between 40 kyr and 8 kyr BP, Nature, 366, 443–445, 1993.

Dreyfus, G. B.: La composition isotopique de l'air piégé dans la glace: interprétation climatique et outil chronologique, Thèse de doctorat de l'Université Pierre et Marie Curie, Paris 6, 1–173, 2008.

Dreyfus, G. B., Parrenin, F., Lemieux-Dudon, B., Durand, G., Masson-Delmotte, V., Jouzel, J., Barnola, J.-M., Panno, L., Spahni, R., Tisserand, A., Siegenthaler, U., and Leuenberger, M.: Anomalous flow below 2700 m in the EPICA Dome C ice core detected using $\delta^{18}O$ of atmospheric oxygen measurements, Clim. Past, 3, 341–353, doi:10.5194/cp-3-341-2007, 2007.

Dunbar, N., McIntosh, W., and Esser, R.: Physical setting and tephrochronology of the summit Caldera ice record at Mount Moulton, West Antarctica, B. Geol. Soc. Am., 7–8, 796–812, 2008.

Durand, G., Svensson, A., Persson, A., Gagliardini, O., Gillet-Chaulet, F., Sjolte, J., Montagnat, M., and Dahl-Jensen, D.: Evolution of the texture along the EPICA Dome C ice core, Physics of ice core records II, T. Hondoh, Hokkaido University Press, 91–106, 2010.

Fujita, S., Okuyama, J., Hori, A. and Hondoh, T., Metamorphism of stratified firn at Dome Fuji, Antarctica: A mechanism for local insolation modulation of gas transport conditions during bubble close off, J. Geophys. Res., 114, F03023, doi:10.1029/2008JF001143, 2009.

Hoffmann, G., Cuntz, M., Weber, C., Ciais, P., Friedlingstein, P., Heimann, M., Jouzel, J., Kaduk, J. Maier-Reimer, E., Seibt, U., and Six, K.: A model of the Earth's Dole effect, Global Biogeochem. Cy., 18, GB1008, doi:10.1029/2003GB002059, 2004.

Huber, C., Beyerle, U., Leuenberger, M., Schwander, J., Kipfer, R., Spahni, R., Severinghaus, J. P., and Weiler, K.: Evidence for molecular size dependent gas fractionation in firn air derived from noble gases, oxygen and nitrogen measurements, Earth Planet. Sc. Lett., 243, 61–73, 2006.

Hutterli, M. A., Schneebeli, M., Freitag, J., Kipfstuhl, J., and Rothlisberger, R.: Impact of local insolation on snow metamorphism and ice core records, Physics of ice core records II, T. Hondoh, Hokkaido University Press, 223–232, 2010.

Ikeda-Fukazawa, T., Fukumizu, K., Kawamura, K., Aoki, S., Nakazawa, T., and Hondoh, T.: Effects of molecular diffusion on trapped gas composition in polar ice cores, Earth Planet. Sc. Lett., 229, 183–192, 2005.

Jouzel, J., Hoffmann, G., Parrenin, F., and Waelbroeck, C.: Atmospheric oxygen 18 and sea-level changes, Quaternary Sci. Rev., 21, 1–3, 2002.

Jouzel, J., Masson-Delmotte, V., Cattani, O., Dreyfus, G., Falourd, S., Hoffmann, G., Minster, B., Nouet, J., Barnola, J.-M., Fisher, H., Gallet, J.-C., Johnsen, S., Leuenberger, M., Loulergue, L., Luethi, D., Oerter, H., Parrenin, F., Raisbeck, G., Raynaud, D., Schilt, A., Schwander, J., Selmo, J., Souchez, R., Spahni, R., Stauffer, B., Steffensen, J. P., Stenni, B., Stocker, T. F., Tison, J.-L., Werner, M., and Wolff, E. W.: Orbital and millennial Antarctic climate variability over the past 800,000 years, Science, 317, 793–796, 2007.

Kawamura, K., Nakazawa, T., Aoki, S., Sugawara, S., Fuji, Y., and Wanatabe, O.: Atmospheric CO_2 variations over the last three glacial-interglacial climatic cycles deduced from the Dome Fuji deep ice core, Antarctica using a wet extraction technique, Tellus B, 55, 126–137, 2003.

Kawamura, K., Parrenin, F., Lisiecki, L., Uemura, R., Vimeux, F., Severinghaus, J. P., Hutterli, M. A., Nakazawa, T., Aoki, S., Jouzel, J., Raymo, M. E., Matsumoto, K., Nakata, H., Motoyama, H., Fujita, S., Goto-Azuma, K., Fujii, K., and Watanabe, O.: Northern hemisphere forcing of climatic cyles over the past 360,000 years implied by accurately dated Antarctic ice cores, Nature, 448, 912–916, 2007.

Landais, A., Caillon, N., Severinghaus, J., Jouzel, J., and Masson-Delmotte, V.: Analyses isotopiques à haute précision de l'air piégé dans les glaces polaires pour la quantification des variations rapides de température: méthodes et limites, Notes des activités instrumentales de l'IPSL, 39, 2003.

Landais, A., Masson-Delmotte, V., Nebout, N., Jouzel, J., Blunier, T., Leuenberger, M., Dahl-Jensen, D., and Johnsen, S.: Millenial scale variations of the isotopic composition of atmospheric oxygen over Marine Isotopic Stage 4, Earth Planet. Sc. Lett., 258, 101–113, doi:10.1016/j.epsl.2007.03.027, 2007.

Landais, A., Dreyfus, D., Capron, E., Sanchez-Goni, M. F., Desprat, S., Jouzel, J., Hoffmann, G., and Johnsen, S.: What drive orbital- and millennial-scale variations of the $\delta^{18}O$ of atmospheric oxygen?, Quaternary Sci. Rev., 29, 235–246, 2010.

Leuenberger, M.: Modeling the signal transfer of seawater $\delta^{18}O$ to the $\delta^{18}O$ of atmospheric oxygen using a diagnostic box model for the terrestrial and marine biosphere, J. Geophys. Res., 102, 26841–26850, 1997.

Lipenkov, V. Ya., Raynaud, D., Loutre, M. F., and Duval, P.: On the potential of coupling air content and O_2/N_2 from trapped air for establishing an ice core chronology based tuned on local insolation, Quaternary Sci. Rev., 30, 3280–3289, doi:10.1016/j.quascirev.2011.07.013, 2011.

Loulergue, L., Schilt, A., Spahni, R., Masson-Delmotte, V., Blunier, T., Lemieux, B., Barnola, J.-M., Raynaud, D., Stocker, T. F., and Chappellaz, J.: Orbital and millennial-scale features of atmospheric CH_4 over the past 800,000 years, Nature, 453, 383–386, 2008.

Loutre, M. F. and Berger, A.: Stage 11 as an analogue for the present interglacial, Global Planet. Change, 36, doi:10.1016/S0921-8181(02)00186-8, 209–217, 2003.

Lüthi, D., Le Floch, M., Bereiter, B., Blunier, T., Barnola, J.-M., Siegenthaler, U., Raynaud, D., Jouzel, J., Fischer, H., Kawamura, K., and Stocker, T. F.: High-resolution carbon dioxide concentration record 650,000–800,000 years before present, Nature, 453, 379–382, 2008.

Malaize, B., Paillard, D., Jouzel, J., and Raynaud, D.: The Dole effect over the last two glacial-interglacial cycles, J. Geophys. Res.-Atmos., 104, 14199–14208, doi:10.1029/1999JD900116, 1999.

Mallat, S.: A wavelet Tour of Signal Processing, Academic Press, San Diego, CA, USA, p.577, 1998.

Martinson, D. G., Pisias, N. G., Hays, J. D., Imbrie, J., Moore, T. C., and Shackleton, N. J.: Age dating and the orbital theory of the ice ages: Development of a high resolution 0 to 300 000 year chronostratigraphy, Quaternary Res., 27, 1–29, 1987.

Melice, J. L. and Servain, J.: The tropical Atlantic meridional SST gradient index and its relationships with the SOI, NAO and Southern Ocean, Clim. Dynam., 20, 447–464, doi:10.1007/s00382-002-0289-x, 2003.

Milankovitch, M. :Kanon der Erdbestrahlung und seine Anwendung auf das Eiszeitenproblem, Royal Serbian Sciences, Spec. pub. 132, section of Mathematical and Natural Sciences, 33, Belgrade, p.633, 1941,

Paillard, D., Labeyrie, L., and Yiou, P.: Macintosh program performs time-series Analysis, Eos Trans. AGU, 77, p.379, 1996.

Parrenin, F., Barnola, J.-M., Beer, J., Blunier, T., Castellano, E., Chappellaz, J., Dreyfus, G., Fischer, H., Fujita, S., Jouzel, J., Kawamura, K., Lemieux-Dudon, B., Loulergue, L., Masson-Delmotte, V., Narcisi, B., Petit, J.-R., Raisbeck, G., Raynaud, D., Ruth, U., Schwander, J., Severi, M., Spahni, R., Steffensen, J. P., Svensson, A., Udisti, R., Waelbroeck, C., and Wolff, E.: The EDC3 chronology for the EPICA Dome C ice core, Clim. Past, 3, 485–497, doi:10.5194/cp-3-485-2007, 2007.

Petit, J. R., Jouzel, J., Raynaud, D., Barkov, N. I., Barnola, J. M., Basile, I., Bender, M., Chappellaz, J., Davis, M., Delaygue, G., Delmotte, M., Kotlyakov, V. M., Legrand, M., Lipenkov, V., Lorius, C., Pepin, L., Ritz, C., Saltzman, E., and Stievenard, M.: Climate and atmospheric history of the past 420 000 years from the Vostok ice core, Nature, 399, 429–436, 1999.

Pol, K., Masson-Delmotte, V., Johnsen, S., Bigler, M., Cattani, O., Durand, G., Falourd, S., Jouzel, J., Minster, B., Parrenin, F., Ritz, C., Steen-Larsen, H. C., and Stenni, B.: New MIS 19 EPICA Dome C high resolution deuterium data: hints for a problematic preservation of climate variability in the "oldest ice", Earth Planet. Sc. Lett., 298, 95–103, doi:10.1016/j.epsl.2010.07.030, 2010.

Raisbeck, G. M., Yiou, F., Jouzel, J., and Stocker, T. F.: Direct north-south synchronization of abrupt climate change record in ice cores using Beryllium 10, Clim. Past, 3, 541–547, doi:10.5194/cp-3-541-2007, 2007.

Rasmussen, S. O., Andersen, K. K., Svensson, A. M., Steffensen, J. P., Vinther, B. M., Clausen, H. B., Andersen, M.-L. S., Johnsen, S. J., Larsen, L. B., Bigler, M., Rothlisberger, R., Fischer, H., Goto-Azuma, K., Hansson, M. E., and Ruth, U.: A new Greenland ice core chronology for the last glacial termination, J. Geophys. Res., 111, D06102, doi:10.1029/2005JD006079, 2006.

Raynaud, D., Lipenkov, V., Lemieux-Dudon, B., Duval, P., Loutre, M.-F., and Lhomme, N.: The local insolation signature of air content in Antarctic ice. A new step toward an absolute dating of

ice records, Earth Planet. Sc. Lett., 261, 337–349, 2007.

Ruddiman, W. F. and Raymo, M. E.: A methane-based time scale for Vostok ice, Quaternary Sci. Rev., 22, 141–155, 2003.

Schmidt, G. A., Shindell, D. T., and Harder, S.: A note on the relationship between ice core methane concentrations and insolation, Geophys. Res. Lett., 31, L23206, doi:10.1029/2004GL021083, 2004.

Severinghaus, J. P. and Battle, M. O.: Fractionation of gases in polar ice during bubble close-off: New constraints from firn air Ne, Kr and Xe observations, Earth Planet. Sc. Lett., 244, 474–500, 2006.

Severinghaus, J. P., Beaudette, R., Headly, M. A., Taylor, K., and Brook, E. J.: Oxygen-18 of O(1) Records the Impact of Abrupt Climate Change on the Terrestrial Biosphere, Science, 324, 1431–1434, doi:10.1126/science.1169473, 2009.

Shackleton, N. J., Hall, M. A., and Vincent, E.: Phase relationships between millennial-scale events 64,000–24,000 years ago, Paleoceanography, 15, 565–569, 2000.

Sowers, T., Bender, M., and Raynaud, D.: Elemental and isotopic composition of occluded O_2 and N_2 in polar ice, J. Geophys. Res., 94, 5137–5150, 1989.

Suwa, M. and Bender, M. L.: Chronology of the Vostok ice core constrained by O_2/N_2 ratios of occluded air, and its implication for the Vostok climate records, Quaternary Sci. Rev., 27, 1093–1106, 2008a.

Suwa, M. and Bender, M. L.: O_2/N_2 ratios of occluded air in the GISP2 ice core, J. Geophys. Res., 113, D11119, doi:11110.11029/12007JD009589, 2008b.

Svensson, A., Andersen, K. K., Bigler, M., Clausen, H. B., Dahl-Jensen, D., Davies, S. M., Johnsen, S. J., Muscheler, R., Rasmussen, S. O., Röthlisberger, R., Steffensen, J. P., and Vinther, B. M.: The Greenland Ice Core Chronology 2005, 15–41 kyr, Part 2: Comparison to other records, Quaternary Sci. Rev., 25, 3258–3267, 2006.

Svensson, A., Andersen, K. K., Bigler, M., Clausen, H. B., Dahl-Jensen, D., Davies, S. M., Johnsen, S. J., Muscheler, R., Parrenin, F., Rasmussen, S. O., Röthlisberger, R., Seierstad, I., Steffensen, J. P., and Vinther, B. M.: A 60 000 year Greenland stratigraphic ice core chronology, Clim. Past, 4, 47–57, doi:10.5194/cp-4-47-2008, 2008.

Torrence, C. and Compo, G. P.: A practical guide to wavelet analysis, B. Am. Meteorol. Soc., 79, 61–78, 1999.

Wang, Y. J., Cheng, H., Edwards, R. L., Kong, X. G., Shao, X. H., Chen, S. T., Wu, J. Y., Jiang, X. Y., Wang, X. F., and An, Z. S.: Millennial- and orbital-scale changes in the East Asian monsoon over the past 224,000 years, Nature, 451, 1090–1093, 2008.

Yiou, F., Raisbeck, G. M., Baumgartner, S., Beer, J., Hammer, C., Johnsen, S., Jouzel, J., Kubik, P. W., Lestringuez, J., Stievenard, M., Suter, M., and Yiou, P.: Beryllium 10 in the Greenland Ice Core Project ice core at Summit, Greenland, J. Geophys. Res., 102, 26783–26794, 1997.

Yuan, D., Cheng, H., Edwards, R. L., Dykoski, C. A., Kelly, M. J., Zhang, M., Qing, J., Lin, Y., Wang, Y., Wu, J., Dorale, J. A., An, Z., and Cai, Y.: Timing, Duration, and Transitions of the Last Interglacial Asian Monsoon, Science, 304, 575–578, 2004.